

SCIENTIFIC REPORTS



OPEN

Unconventional superconductivity and interaction induced Fermi surface reconstruction in the two-dimensional Edwards model

Received: 22 December 2015

Accepted: 15 February 2016

Published: 03 March 2016

Dai-Ning Cho¹, Jeroen van den Brink¹, Holger Fehske², Klaus W. Becker³ & Steffen Sykora¹

We study the competition between unconventional superconducting pairing and charge density wave (CDW) formation for the two-dimensional Edwards Hamiltonian at half filling, a very general two-dimensional transport model in which fermionic charge carriers couple to a correlated background medium. Using the projective renormalization method we find that a strong renormalization of the original fermionic band causes a new hole-like Fermi surface to emerge near the center of the Brillouin zone, before it eventually gives rise to the formation of a charge density wave. On the new, disconnected parts of the Fermi surface superconductivity is induced with a sign-changing order parameter. We discuss these findings in the light of recent experiments on iron-based oxypnictide superconductors.

In a number of superconducting (SC) materials the pairing interaction is not predominantly mediated by phonons, but rather by electron-electron interactions, for instance in the guise of spin fluctuations in the recently discovered extended family of iron-based superconductors^{1–3}. Electron-electron interactions, however, are also driving the metallic ground state towards other long-range ordered states, in particular spin^{4,5}- or charge-density waves^{6–8} (CDWs). A minimal model to effectively describe these interactions considers fermionic charge carriers in the presence of a correlated background that is provided by bosonic modes in the particle's immediate vicinity which take an active part in the transport of the fermions⁹. Such a picture is very general with wide applicability, for example to the case of charge transport in high-temperature SC materials^{10–12} where superconductivity appears close to magnetically ordered phases¹³.

The fundamental question arises whether there is a SC state where the Cooper pairing is solely based on electron-electron interaction and in particular whether and how such a phase competes with other ordered states mediated by the same generic background correlations. An effective lattice model which mimics quantum transport in a correlated background is the Edwards fermion-boson model¹⁴,

$$\mathcal{H}/t_b = -\sum_{\langle i,j \rangle} c_j^\dagger c_i (b_i^\dagger + b_j) - \Lambda \sum_i (b_i^\dagger + b_i) + \Omega \sum_i b_i^\dagger b_i, \quad (1)$$

which is here considered for a 2D square lattice. It describes the hopping of spinless fermions between nearest-neighbor sites i and j affected by a correlated background medium modelled by bosonic degrees of freedom. Local excitations and quantum fluctuations in the background medium are parametrized by dimensionless parameters Ω and Λ , which give the energy cost of a bosonic excitation and the ability of the background to relax, respectively. Originally, the Edwards model was introduced to describe the motion of a spinless particle in an antiferromagnetic correlated spin background - like a hole in the t - J model. In this context the Edwards model is relevant to charge transport in high-temperature superconductors at doping levels close to an antiferromagnetically ordered state¹⁵ but also in other materials with related models with spin degrees of freedom¹⁶. The advantage of the Edwards model is that the correlated spin background is parametrized by bosonic degrees of freedom, which might be represented, for example, by Schwinger bosons. Thus, in the Edwards model the charge

¹IFW Dresden, P.O. Box 270116, 01171 Dresden, Germany. ²Institut für Physik, Ernst-Moritz-Arndt-Universität Greifswald, D-17487 Greifswald, Germany. ³Institut für Theoretische Physik, Technische Universität Dresden, D-01062 Dresden, Germany. Correspondence and requests for materials should be addressed to S.S. (email: s.sykora@ifw-dresden.de)

carriers are modelled by spinless fermions, whereas the background spin correlations are represented by bosons. Therefore, the 2D Edwards Hamiltonian (1) also allows the study of superconductivity using spinless fermions and the spin degrees of freedom are modelled by bosons in a way described above.

Shortly after its introduction the model (1) was solved numerically for a single particle in 1D by a variational diagonalization technique¹⁵, and in 2D treated approximatively by the momentum-average approach¹⁷. The many-particle case has been studied intensively for the 1D system within DMRG, where a surprisingly rich phase diagram has been found, including metallic repulsive and attractive Tomonaga-Luttinger-liquid phases, insulating CDW states at half-filling^{18,19} and one-third-filling²⁰, and regions with phase separation²¹.

In this work, we exploit the projective renormalization method (PRM)²² to the Edwards model at half-filling and find an intricate interplay between stable superconducting and charge-density wave states, that strongly depends on the excitation energy of the correlated background medium. The original fermionic band is strongly renormalized by the coupling to the bosonic modes, which can give rise to an entirely new hole-like part of the Fermi surface (FS) close to the center of the Brillouin zone. The superconducting order parameter has a different sign on the two disconnected parts of the FS that subsequently emerge. Such an interaction induced Fermi surface reconstruction has been observed in recent experiments on oxypnictide superconductors where indeed also sign-changing s_{\pm} superconductivity is present.

Before discussing the results of our many-particle method for the Edwards model in 2D we start with an appropriate reformulation of Hamiltonian (1) in such a way that a coupled system of free fermions and bosons is obtained. Fourier transformation, introduction of fluctuation operators for fermions, and elimination of the linear term of bosonic operators as shown in ref. 19 allows the following decomposition $\mathcal{H} = \mathcal{H}_0 + \mathcal{H}_1$ in momentum space,

$$\mathcal{H}_0 = \sum_{\mathbf{k}} \varepsilon_{\mathbf{k}} \delta(c_{\mathbf{k}}^{\dagger} c_{\mathbf{k}}) + \Omega t_b \sum_{\mathbf{q}} b_{\mathbf{q}}^{\dagger} b_{\mathbf{q}} - N \frac{\Omega t_f^2}{4t_b}, \quad (2)$$

$$\mathcal{H}_1 = \frac{1}{\sqrt{N}} \sum_{\mathbf{k}\mathbf{q}} g_{\mathbf{k}} \left[b_{\mathbf{q}}^{\dagger} \delta(c_{\mathbf{k}}^{\dagger} c_{\mathbf{k}+\mathbf{q}}) + b_{\mathbf{q}} \delta(c_{\mathbf{k}+\mathbf{q}}^{\dagger} c_{\mathbf{k}}) \right], \quad (3)$$

where $\varepsilon_{\mathbf{k}} = -2t(\cos k_x a + \cos k_y a)$, $g_{\mathbf{k}} = -2t_b(\cos k_x a + \cos k_y a)$, and $t = (2t_b/\Omega)[\Lambda - (1/N) \sum_{\mathbf{k}} (g_{\mathbf{k}}/t_b) \langle c_{\mathbf{k}}^{\dagger} c_{\mathbf{k}} \rangle]$. Here a is the lattice constant of the 2D square lattice with N sites. Fluctuation operators $\delta(c_{\mathbf{k}}^{\dagger} c_{\mathbf{k}+\mathbf{q}}) = c_{\mathbf{k}}^{\dagger} c_{\mathbf{k}+\mathbf{q}} - \langle c_{\mathbf{k}}^{\dagger} c_{\mathbf{k}+\mathbf{q}} \rangle$ were introduced in order to attribute the mean-field contributions to the free term \mathcal{H}_0 , which simplifies the solution of the many-body problem by the projective renormalization method (PRM).

Results

One of the main aims of our work is to discuss the question whether the Edwards model provides an attractive pairing interaction. If so, we have to clarify its structure in momentum space and in which parameter space the SC phase is stable with respect to other ordered states. To reveal a possible SC pairing mechanism an approximate BCS-like relation between the SC order parameter and pairing correlation function can be derived from the PRM renormalization equations, $\tilde{\Delta}_{\mathbf{k}} \approx (1/N) \sum_{\mathbf{q}} V_{\mathbf{k},\mathbf{q}} \langle c_{-\mathbf{q}} c_{\mathbf{q}} \rangle$, where $V_{\mathbf{k},\mathbf{q}}$ is an approximate analytic expression for the momentum-dependent pairing potential, $V_{\mathbf{k},\mathbf{q}} = -4g_{\mathbf{k}} g_{\mathbf{k}+\mathbf{q}} \tilde{\omega}_{\mathbf{q}} / [\tilde{\omega}_{\mathbf{q}}^2 - (\tilde{\varepsilon}_{\mathbf{k}} - \tilde{\varepsilon}_{\mathbf{k}+\mathbf{q}})^2]$. The momentum-dependent quantities $\tilde{\varepsilon}_{\mathbf{k}}$ and $\tilde{\omega}_{\mathbf{q}}$ are determined self-consistently by the PRM approach and they describe the fully renormalized one-particle energies of the fermions and bosons, respectively (compare Eq. (5) from the Methods section). According to the prefactor $g_{\mathbf{k}} = -2t_b(\cos k_x a + \cos k_y a)$, the pairing potential becomes strongly momentum-dependent with a sign-change indicating an unconventional Cooper pairing mechanism.

We have evaluated the PRM renormalization equations in the half-filled band case, i.e. for $N_e/N = 0.5$, where N_e is the number of fermionic particles, and have varied the parameter Ω . The second parameter Λ was fixed to a very small value $\Lambda = 0.001$ describing a rather stiff, strongly correlated background which supports the formation of ordered states, as for example the SC and CDW states. As a result we found that the 2D Edwards model forms three different ground states. A metallic state at small values of Ω , a SC state in a narrow region for intermediate values of the bosonic energy, $\Omega \approx 2.8 \cdots 3.5$, and a quantum phase transition to a CDW state for large values of Ω , which is a characteristic ground state in the limit of large background excitations energies.

In Fig. 1(a) a SC solution at $\Omega = 3.27$ is shown. Here the SC pairing correlation function $\langle c_{-\mathbf{k}} c_{\mathbf{k}} \rangle$ and the pairing potential $V_{\mathbf{k}=0,\mathbf{q}}/t_b$ are given along momentum cuts in the main symmetry directions. Most notably, we find a pronounced tendency towards electron pairing in a certain momentum region around the Γ point $\mathbf{k} = (0, 0)$, where also an attractive pairing potential evolves. As is shown further below, the SC state is accompanied by the appearance of a new Fermi surface formed around the Γ point in the course of band renormalization, which appears for a specific range of Ω values. Note that the pairing potential is also negative around (π, π) , where, however, SC pairing is suppressed due to the absence of fermionic low-energy states. The jump in the pairing potential appearing in Fig. 1(a) at momenta where $\tilde{\varepsilon}_{\mathbf{k}} \approx \tilde{\omega}_{\mathbf{q}}$ is an artifact of the specific perturbative shape of $V_{\mathbf{k},\mathbf{q}}$. In the actual calculations this divergency is removed by renormalization contributions up to infinite order in $g_{\mathbf{k}}$.

Figure 1(b) shows solutions of the renormalized SC and CDW order parameters $\Delta_{\mathbf{k}_F}^{SC} = \tilde{\Delta}_{\mathbf{k}_F}^{SC}$ and $\Delta_{\mathbf{k}_F}^{CDW} = \tilde{\Delta}_{\mathbf{k}_F}^{CDW}$ (\mathbf{k}_F : Fermi momentum) as a function of Ω . Thereby the normalization factors BW in Fig. 1(b) are the band widths of the corresponding renormalized fermionic quasiparticle bands.

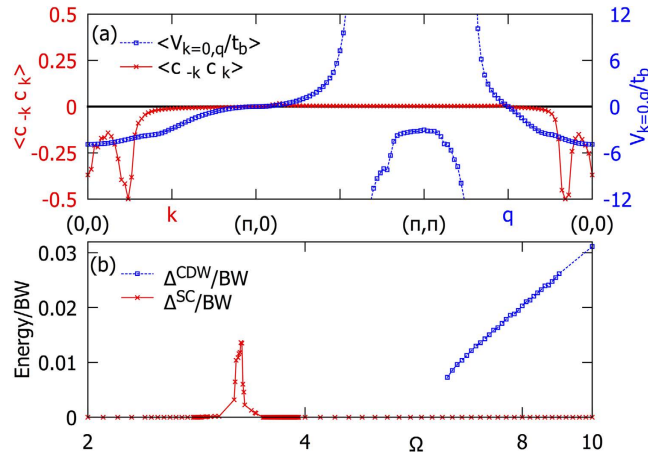


Figure 1. Panel (a): Momentum cuts along the symmetry directions $\Gamma \Rightarrow X \Rightarrow M \Rightarrow \Gamma$ in the SC regime at $\Omega = 3.27$ for the pairing correlation function $\langle c_{-k} c_k \rangle$ (left axis) and approximate pairing potential $V_{k,q}/t_b$ (right axis) where \mathbf{k} is set to $\mathbf{k} = (0, 0)$. The pairing potential is negative in a certain region around the Γ -point leading to attractive pairing inside the inner hole pocket which is indicated by a non-zero pairing correlation function. Panel (b): Renormalized SC order parameter Δ^{SC} (red solid line) and charge-density wave order parameter Δ^{CDW} (blue dashed line) as a function of the bosonic energy Ω . The order parameter values are related to the respective band widths (BW) of the renormalized fermionic bands for the two cases. The lattice grid is 100×100 and the temperature is set to zero.

To characterize the three phases in more detail, in Fig. 2 we have considered the fully renormalized one-particle energies $\tilde{\epsilon}_k$ (left panels) and $\tilde{\omega}_q$ (right panels) in the entire Brillouin zone. First, for a small value $\Omega = 2$, we find typical metallic behavior with a strong dispersion $\tilde{\epsilon}_k$, which corresponds to the quasiparticle energy. For larger values of Ω , $\tilde{\epsilon}_k$ changes dramatically as can be seen for $\Omega = 3.27$. In this regime, the bosonic energy is in the same order as the renormalized fermionic bandwidth. Moreover, $\tilde{\epsilon}_k$ is shifted to values very close to the Fermi level in a certain region in momentum space. The strong renormalization leads to a new hole-like Fermi surface appearing at momentum $k_F \approx 0.16\pi$, which describes an unoccupied area around the Γ point. According to Fig. 1(a) the states inside this region have been detected to be responsible for the formation of the SC state. However, the low-energy states along the outer Fermi surface are not involved in the SC pairing, because there the pairing potential is zero. For the same reason, combinations of inter-pocket scattering vectors between inner and outer Fermi surface parts do not contribute to the pairing. For still larger Ω inside the CDW regime the SC state is suppressed, due to the absence of a Fermi surface in a momentum region with negative pairing potential. As in the metallic state, the normal state Fermi surface runs along the line where g_k is zero, leading to a suppression of the pairing potential.

For the SC gap we find constant values along the two Fermi surface parts and a characteristic sign change between them. At $\Omega = 3.27$ we have computed the values $\Delta_1 = 1.3 \cdot 10^{-2}$ and $\Delta_2 = -2.0 \cdot 10^{-4}$ (in terms of the renormalized bandwidth) for the inner hole pocket and the outer part, respectively. Thus, along the outer Fermi surface the gap value is non-zero but very small, $|\Delta_2| \ll |\Delta_1|$, which suppresses the pairing function $\langle c_{-k} c_k \rangle$ in Fig. 1(a) upon crossing the outer Fermi surface. The sign-change on disconnected parts of the Fermi surface, with s -wave pairing on each disjunct part is often denoted as s_{\pm} superconductivity in the context of iron-based pnictide superconductors²³. The remarkable feature in the half-filled Edwards model is not as much the s_{\pm} symmetry of the superconducting order parameter, but rather that the interactions induce a change in the topology of the Fermi surface – a Lifshitz transition. Such an interaction-induced Fermi-surface reconstruction was recently observed in a prototypical compound 1111-type iron-based oxypnictide superconductor, $\text{SmFe}_{0.92}\text{Co}_{0.08}\text{AsO}$, which has a T_c of 55 K. Angle resolved photoemission (ARPES) experiments show that its Fermi surface is reconstructed by the edges of several bands that are pulled to the Fermi level from the depths of the theoretical band structure²⁴. This type of Fermi surface reconstruction is argued to be correlated with the maximally attainable superconducting transition temperature in iron-based superconductors. In particular our observation of a rather high density of states in the vicinity of the inner hole pocket giving rise to the strong Cooper pairing around the Γ point is consistent with these ARPES results.

For larger $\Omega > 4.19$ the hole-like Fermi surface disappears again. For $\Omega > 6.2$ we find a CDW ordered state characterized by a gap in the fermionic quasiparticle spectrum. A representative CDW solution is shown in Fig. 2 at $\Omega = 8$ (left panel). The gap opens along the black solid line connecting the momentum vectors $(0, \pm\pi)$ and $(\pm\pi, 0)$ and is reflected in a jump of the color code. Note that between $\Omega \approx 3.5$ and $\Omega \approx 6.1$ no stable CDW solution was found so that no reliable statement can be given for this interval.

Finally, let us characterize the different regimes from the viewpoint of the background correlations. In Fig. 2 (right panel) the renormalized bosonic energy $\tilde{\omega}_q/(\Omega t_b)$ describes the excitations in the background which have acquired a dispersion from the coupling to the fermions. This renormalization is a consequence of an effective non-local interaction between bosons, which is mediated by higher-order contributions in the fermion-boson coupling. As a result the frequency of the boson either increases (hardens) or decreases (weakens). However, a

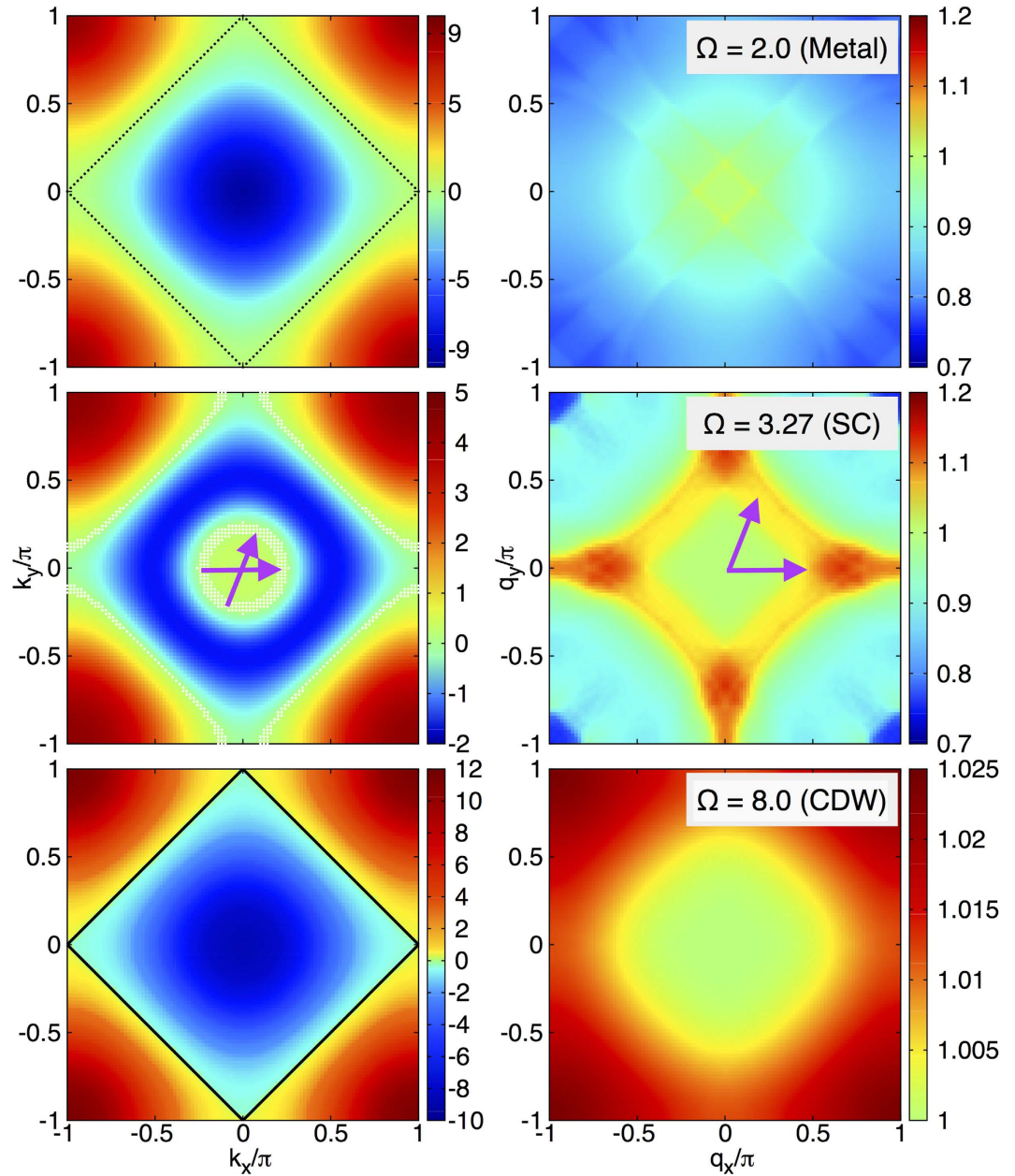


Figure 2. Fully renormalized quasiparticle energies $\tilde{\epsilon}_k/t_b = \epsilon_{\mathbf{k},\lambda=0}/t_b$ (left panels) and $\tilde{\omega}_q/(\Omega t_b) = \omega_{\mathbf{q},\lambda=0}/(\Omega t_b)$ (right panels) of fermions and bosons in the 2D square lattice Brillouin zone for $\Lambda = 0.001$ and different values of Ω . Ωt_b is the bare bosonic energy. The Fermi surface (black dotted line) and the strong dispersion of $\tilde{\epsilon}_k/t_b$ indicate metallic behavior at $\Omega = 2$. In the SC state ($\Omega = 3.27$) the momentum dependence of $\tilde{\epsilon}_k/t_b$ changes qualitatively, forming a new hole-like Fermi surface around the center of the Brillouin zone. The momentum vectors with $|\tilde{\epsilon}_k| < \Delta^{SC}$ (white dots), where Δ^{SC} is the SC gap, indicate the position of the respective normal state Fermi surface. It is split into two disconnected parts. Arrows mark representative dominant processes stabilizing the SC state by virtual bosons. For $\Omega = 8$ a CDW state is found. The formation of the CDW gap is indicated by the black lines, which also encompass the reduced Brillouin zone in the CDW phase. The remaining area describes the second quasiparticle band which can be back folded by the CDW ordering vector $\mathbf{Q} = (\pi, \pi)$ to the reduced Brillouin zone.

real soft-mode behavior as it is discussed for instance in the context of structural phase transitions is not observed in the Edwards model in any parameter regime. First, the metallic state ($\Omega = 2.0$) is characterized by a lowering of the effective background energy indicating an attractive Fermi liquid. Here the transport is accompanied by a ‘cloud’ of bosonic excitations similar to the large polaron formation in the presence of phonons. In particular, in the SC state ($\Omega = 3.27$) an interesting structure of the background energy distribution is found in momentum space. The figure shows that $\tilde{\omega}_q$ increases inside a Brillouin zone region (green and yellow color), which is bounded by scattering vectors \mathbf{q} that roughly fulfill the resonance condition $|\tilde{\epsilon}_k - \tilde{\epsilon}_{\mathbf{k}+\mathbf{q}}| \approx \tilde{\omega}_q$. This leads to

a large renormalization with a characteristic change from hardening to weakening. Such a behavior is also seen in the jump of the pairing potential in Fig. 1(b) which, however, appears at different momentum vectors due to the fixed \mathbf{k} vector. Inside the boson hardening region we can identify the momentum vectors of the particular bosons which are involved in the SC pairing (represented by two purple arrows in Fig. 2). They connect states inside the new inner hole pocket where the pairing correlation function is non-zero. Finally, in the CDW regime ($\Omega = 8.0$) the weakening area disappears completely and no states are available to form Cooper pairs. Here $\tilde{\omega}_q/(\Omega t_b) > 1$ throughout the Brillouin zone and the momentum dependence of the background excitation energy is inverted with respect to the metallic state emphasizing strongly repulsive particle-particle interaction, leading immediately to a breakup of any pairing. The hardening is a characteristic feature of the CDW phase and has already been found in 1D¹⁹.

Conclusions

We have studied the interplay between unconventional superconductivity and CDW order within a generic fermion-boson transport model in 2D. In the half-filled case stable SC solutions besides a CDW state were found. The SC state is stabilized by an attractive pairing on an additional hole-like Fermi surface around the center of the Brillouin zone which arises through a strong renormalization of the bare fermionic bandstructure. The highly unconventional pairing mechanism is due to interaction processes of infinite order in the coupling $g_{\mathbf{k}}$ between spinless fermions and background correlations, leading to a momentum-dependent pairing potential which forms a SC state with possible variation of the order parameter phase. Fourier transformation of the $\tilde{\Delta}_{\mathbf{k}}$ solution to real space leads to a rather local pairing between next nearest lattice sites. It follows that the character of the SC pairing is influenced by fluctuations of the competing charge ordered state. These results are highly relevant for the currently investigated iron-based oxypnictides.

Methods

Following the basic idea of ref. 19 the interaction part \mathcal{H}_1 , given by Eq. (3), is integrated out by a series of unitary transformations starting from large to zero transition energies. Assuming that all transitions with energies larger than some energy cutoff λ have already been integrated out, the transformed Hamiltonian \mathcal{H}_λ consists of a part which has the same operator structure as Eqs (2) and (3), but with λ -dependent parameters, and an additional term of the form $\sum_{\mathbf{k}} [\Delta_{\mathbf{k},\lambda} c_{\mathbf{k}}^\dagger c_{-\mathbf{k}} + \Delta_{\mathbf{k},\lambda}^* c_{-\mathbf{k}} c_{\mathbf{k}}]$ allowing for possible SC solutions based on an unconventional Cooper pairing of spinless fermions.

Evaluating the unitary transformation up to order $g_{\mathbf{k}}^2$, discrete renormalization equations for all λ -dependent parameters are obtained, which connect the parameters at cutoff λ with those at $\lambda - \Delta\lambda$. The discrete renormalization equation for the SC order parameter function reads

$$\Delta_{\mathbf{k},\lambda-\Delta\lambda} - \Delta_{\mathbf{k},\lambda} = -\frac{2g_{\mathbf{k}}}{N} \sum_{\mathbf{q}} g_{\mathbf{k}+\mathbf{q}} \langle c_{-(\mathbf{k}+\mathbf{q})} c_{\mathbf{k}+\mathbf{q}} \rangle \times \left(\frac{\Theta_{\mathbf{k},\mathbf{q},\lambda}^{\Delta\lambda} \Theta_{\mathbf{k}+\mathbf{q},-\mathbf{q},\lambda}}{\varepsilon_{\mathbf{k},\lambda} - \varepsilon_{\mathbf{k}+\mathbf{q},\lambda} + \omega_{\mathbf{q},\lambda}} + \frac{\Theta_{\mathbf{k},\mathbf{q},\lambda} \Theta_{\mathbf{k}+\mathbf{q},-\mathbf{q},\lambda}^{\Delta\lambda}}{\varepsilon_{\mathbf{k}+\mathbf{q},\lambda} - \varepsilon_{\mathbf{k},\lambda} + \omega_{\mathbf{q},\lambda}} \right), \quad (4)$$

where the Θ -functions $\Theta_{\mathbf{k},\mathbf{q},\lambda}^{\Delta\lambda} = \Theta_{\mathbf{k},\mathbf{q},\lambda} (1 - \Theta_{\mathbf{k},\mathbf{q},\lambda-\Delta\lambda})$ with $\Theta_{\mathbf{k},\mathbf{q},\lambda} = \Theta(\lambda - |\varepsilon_{\mathbf{k},\lambda} - \varepsilon_{\mathbf{k}+\mathbf{q},\lambda} + \omega_{\mathbf{q},\lambda}|)$ restrict the momentum sum to excitation energies within a small energy shell $\Delta\lambda$. This allows to apply perturbation theory in each small renormalization step. However, the overall renormalization is far beyond perturbation theory and renormalization processes to infinite order in the coupling $g_{\mathbf{k}}$ are taken into account. Furthermore, note that in each single renormalization step a factorization approximation leads to the appearance of expectation values in the renormalization equations¹⁹.

The renormalization approach starts by reducing λ in steps $\Delta\lambda$ until $\lambda = 0$ is reached. This is achieved by numerical evaluation of the renormalization equations. Then, all transitions from \mathcal{H}_1 are used up and the fully renormalized Hamiltonian $\tilde{\mathcal{H}} = \mathcal{H}_{\lambda=0}$ describes an uncoupled system of bosons and spinless fermions, which can be SC ($\tilde{\Delta}_{\mathbf{k}} \neq 0$) depending on the chosen initial parameter set: The fully renormalized Hamiltonian reads

$$\tilde{\mathcal{H}} = \sum_{\mathbf{k}} [\tilde{\varepsilon}_{\mathbf{k}} c_{\mathbf{k}}^\dagger c_{\mathbf{k}} + (\tilde{\Delta}_{\mathbf{k}} c_{\mathbf{k}}^\dagger c_{-\mathbf{k}} + \text{h.c.})] + \sum_{\mathbf{q}} \tilde{\omega}_{\mathbf{q}} b_{\mathbf{q}}^\dagger b_{\mathbf{q}}. \quad (5)$$

The PRM described in ref. 19 also allows the calculation of expectation values, $\langle \mathcal{A} \rangle = \langle \tilde{\mathcal{A}} \rangle_{\tilde{\mathcal{H}}}$, where $\tilde{\mathcal{A}}$ is the fully renormalized quantity using the same set of unitary transformations as for $\tilde{\mathcal{H}}$. An example is the pairing expectation value $\langle c_{-\mathbf{k}} c_{\mathbf{k}} \rangle$ from Eq. (4). In a second step the renormalization procedure starts again with the improved expectation values $\langle c_{-\mathbf{k}} c_{\mathbf{k}} \rangle$ by reducing again the cutoff from its maximum value $\tilde{\lambda}$ to $\lambda = 0$. After a sufficient number of such cycles, the expectation values are converged and the renormalization equation (4) is solved self-consistently. Besides SC order we also take into account a possible CDW order (not included in Eq. (5)), a phase that is expected to be present at half-filling^{18,19}.

References

1. Mazin, I. I., Singh, D. J., Johannes, M. D. & Du, M. H. Unconventional Superconductivity with a Sign Reversal in the Order Parameter of LaFeAsO_{1-x}F_x. *Phys. Rev. Lett.* **101**, 057003 (2008).
2. Kuroki, K. *et al.* Unconventional Pairing Originating from the Disconnected Fermi Surfaces of Superconducting LaFeAsO_{1-x}F_x. *Phys. Rev. Lett.* **101**, 087004 (2008).
3. Tsuei, C. C. & Kirtley, J. R. Pairing symmetry in cuprate superconductors. *Rev. Mod. Phys.* **72**, 969 (2000).

4. Millis, A. J., Schofield, A. J., Lonzarich, G. G. & Grigera, S. A. Metamagnetic Quantum Criticality in Metals. *Phys. Rev. Lett.* **88**, 217204 (2002).
5. Lester, C. *et al.* Field-tunable spin-density-wave phases in $\text{Sr}_3\text{Ru}_2\text{O}_7$. *Nature Materials* **14**, 373 (2015).
6. Johannes, M. D. & Mazin, I. I. Fermi surface nesting and the origin of charge density waves in metals. *Phys. Rev. B* **77**, 165135 (2008).
7. Hellmann, S. *et al.* Time-domain classification of charge-density-wave insulators. *Nature Communications* **3**, 1069 (2012).
8. Watanabe, H., Seki, K. & Yunoki, S. Charge-density wave induced by combined electron-electron and electron-phonon interactions in 1T-TiSe_2 : A variational Monte Carlo study. *Phys. Rev. B* **91**, 205135 (2015).
9. Berciu, M. Viewpoint: Challenging a hole to move through an ordered insulator. *Physics* **2**, 55 (2009).
10. Wu, T. *et al.* Magnetic-field-induced charge-stripe order in the high-temperature superconductor $\text{YBa}_2\text{Cu}_3\text{O}_y$. *Nature* **477**, 191 (2011).
11. Chang, J. *et al.* Direct observation of competition between superconductivity and charge density wave order in $\text{YBa}_2\text{Cu}_3\text{O}_{6.67}$. *Nature Physics* **8**, 871 (2012).
12. Ghiringhelli, G. *et al.* Long-Range Incommensurate Charge Fluctuations in $(\text{Y,Nd})\text{Ba}_2\text{Cu}_3\text{O}_{6+x}$. *Science* **337**, 821 (2012).
13. Wohlfeld, K., Oles, A. M. & Horsch, P. Orbital induced string formation in the spin-orbital polarons. *Phys. Rev. B* **79**, 224433 (2009).
14. Edwards, D. M. A quantum phase transition in a model with boson-controlled hopping. *Physica B* **378–380**, 133 (2006).
15. Alvermann, A., Edwards, D. M. & Fehske, H. Boson-Controlled Quantum Transport. *Phys. Rev. Lett.* **98**, 056602 (2007).
16. Edwards, D. M., Ejima, S., Alvermann, A. & Fehske, H. A Green's function decoupling scheme for the Edwards fermion-boson model. *Journal of Physics: Condensed Matter* **22**, 435601 (2010).
17. Berciu, M. & Fehske, H. Momentum average approximation for models with boson-modulated hopping: Role of closed loops in the dynamical generation of a finite quasiparticle mass. *Phys. Rev. B* **82**, 085116 (2010).
18. Ejima, S., Hager, G. & Fehske, H. Quantum Phase Transition in a 1D Transport Model with Boson-Affected Hopping: Luttinger Liquid versus Charge-Density-Wave Behavior. *Phys. Rev. Lett.* **102**, 106404 (2009).
19. Sykora, S., Becker, K. W. & Fehske, H. Charge-density-wave formation in a half-filled fermion-boson transport model: A projective renormalization approach. *Phys. Rev. B* **81**, 195127 (2010).
20. Ejima, S. & Fehske, H. Charge-Density-Wave Formation in the Edwards Fermion-Boson Model at One-Third Band Filling. *JPS Conf. Proc.* **3**, 013006 (2014).
21. Ejima, S., Sykora, S., Becker, K. W. & Fehske, H. Phase separation in the Edwards model. *Phys. Rev. B* **86**, 155149 (2012).
22. Becker, K. W., Hübsch, A. & Sommer, T. Renormalization approach to many-particle systems. *Phys. Rev. B* **66**, 235115 (2002).
23. Johnston, D. C. The puzzle of high temperature superconductivity in layered iron pnictides and chalcogenides. *Adv. Phys.* **59**, 803 (2010).
24. Charnukha, A. *et al.* Interaction-induced singular Fermi surface in a high-temperature oxypnictide superconductor. *Sci. Rep.* **5**, 10392 (2015).

Acknowledgements

We would like to thank S. Ejima, G. Hager, K. Koepnick, and D. Efremov for helpful discussions. This work was supported by Deutsche Forschungsgemeinschaft through the Collaborative Research Center SFB 1143, and SFB 652 B5 (H.F.).

Author Contributions

S.S. and H.F. initiated the project. D.-N.C. and S.S. developed the theory. D.-N.C. performed the numerical calculations. S.S., H.F., K.W.B. and J.v.d.B. wrote the main manuscript text and D.-N.C. and S.S. prepared the figures. All authors discussed the results and reviewed the manuscript.

Additional Information

Competing financial interests: The authors declare no competing financial interests.

How to cite this article: Cho, D.-N. *et al.* Unconventional superconductivity and interaction induced Fermi surface reconstruction in the two-dimensional Edwards model. *Sci. Rep.* **6**, 22548; doi: 10.1038/srep22548 (2016).



This work is licensed under a Creative Commons Attribution 4.0 International License. The images or other third party material in this article are included in the article's Creative Commons license, unless indicated otherwise in the credit line; if the material is not included under the Creative Commons license, users will need to obtain permission from the license holder to reproduce the material. To view a copy of this license, visit <http://creativecommons.org/licenses/by/4.0/>